

Quantum Discrete Cosine Transform for Image Compression

Chao-Yang Pang^{1,2,*}, Zheng-Wei Zhou^{1,†} and Guang-Can Guo^{1‡}

*Key Laboratory of Quantum Information,
University of Science and Technology of China,
Chinese Academy of Sciences, Hefei, Anhui 230026, China¹
College of Mathematics and Software Science,
Sichuan Normal University, Chengdu,
Sichuan 610066, People's Republic of China²*

Abstract

Discrete Cosine Transform (DCT) is very important in image compression. Classical 1-D DCT and 2-D DCT has time complexity $O(N \log_2 N)$ and $O(N^2 \log_2 N)$ respectively. This paper presents a quantum DCT iteration, and constructs a quantum 1-D and 2-D DCT algorithm for image compression by using the iteration. The presented 1-D and 2-D DCT has time complexity $O(\sqrt{N})$ and $O(N)$ respectively. In addition, the method presented in this paper generalizes the famous Grover's algorithm to solve complex unstructured search problem.

*Electronic address: cyp'900@hotmail.com

†Electronic address: zwzhou@ustc.edu.cn

‡Electronic address: gcguo@ustc.edu.cn

I. INTRODUCTION

A. The Conception of Digital Image

The result of sampling and quantization of a monochromic N-by-N image is a matrix of real numbers[1, 2]

$$F = \begin{bmatrix} f_{00} & f_{01} & \cdots & f_{0(N-1)} \\ f_{10} & f_{11} & \cdots & f_{1(N-1)} \\ \vdots & \vdots & \vdots & \vdots \\ f_{(N-1)0} & f_{(N-1)1} & \cdots & f_{(N-1)(N-1)} \end{bmatrix} \quad (1)$$

Each element of this matrix is called *pixel*. The pixel f_{ij} is a gray-level value. The value f_{ij}^2 is proportional to brightness or energy.

Let column vector

$$\vec{f}_i = (f_{0i}, f_{1i}, \dots, f_{(N-1)i})^T \quad (2)$$

, where T represents the transpose of a vector.

The digital image F can be expressed as formula

$$F = \left[\begin{array}{c} \vec{f}_0 \\ \vec{f}_1 \\ \dots \\ \vec{f}_{N-1} \end{array} \right] \quad (3)$$

Fig. 1 illustrates the conception of digital image.

Insert Fig1 Here

B. Introduction of Classical Discrete Cosine Transform (DCT)

1. One-Dimensional Discrete Cosine Transform (1-D DCT)

The one-dimensional discrete cosine transform[1, 2] (1-D DCT) and inverse DCT are defined as

$$\begin{cases} c_u = \sum_{n=0}^{N-1} \alpha_u f_n \cos \frac{(2n+1)u\pi}{2N} \\ f_n = \sum_{u=0}^{N-1} a_u c_u \cos \frac{(2n+1)u\pi}{2N} \end{cases} \quad (4)$$

$(0 \leq u, n \leq N - 1)$

, where

$$\alpha_u = \begin{cases} 1/\sqrt{N} & \text{if } u = 0 \\ \sqrt{2/N} & \text{if } 1 < u < N \end{cases}$$

The $N \times N$ DCT matrix is

$$D = (\alpha_u \cos \frac{(2n+1) \times u\pi}{2N})_{N \times N} = \begin{bmatrix} \alpha_0 & \cdots & \alpha_0 \\ \alpha_1 \cos \frac{1 \times 1\pi}{2N} & \cdots & \alpha_1 \cos \frac{(2N-1) \times 1\pi}{2N} \\ \vdots & \cdots & \vdots \\ \alpha_{N-1} \cos \frac{1 \times (N-1)\pi}{2N} & \cdots & \alpha_{N-1} \cos \frac{(2N-1) \times (N-1)\pi}{2N} \end{bmatrix} \quad (5)$$

Let vector

$$\vec{D}_u = \alpha_u (\cos \frac{1 \cdot u\pi}{2N}, \cos \frac{3 \cdot u\pi}{2N}, \dots, \cos \frac{(2N-1) \cdot u\pi}{2N})^T \quad (6)$$

, where $0 \leq u < N$

The $N \times N$ DCT matrix can be expressed as

$$D = (\alpha_u \cos \frac{(2n+1)u\pi}{2N})_{N \times N} = \begin{bmatrix} (\vec{D}_0)^T \\ (\vec{D}_1)^T \\ \vdots \\ (\vec{D}_{N-1})^T \end{bmatrix} \quad (7)$$

Equation (4) can be expressed as

$$\vec{c} = \begin{pmatrix} c_0 \\ c_1 \\ \vdots \\ c_{N-1} \end{pmatrix} = D \vec{f} = \begin{pmatrix} \vec{D}_0 \bullet \vec{f} \\ \vec{D}_1 \bullet \vec{f} \\ \vdots \\ \vec{D}_{N-1} \bullet \vec{f} \end{pmatrix} \quad (8)$$

where “ \bullet ” expresses inner product between two vectors.

2. Two-Dimensional Discrete Cosine Transform (2-D DCT)

The definition of the two-dimensional DCT [1, 2] (2-D DCT) for input image F and coefficients matrix C (output) is

$$\begin{cases} c_{pq} = \alpha_p \alpha_q \sum_{m=0}^{N-1} \sum_{n=0}^{N-1} f_{mn} \cos \frac{\pi(2m+1)p}{2N} \cos \frac{\pi(2n+1)q}{2N} \\ f_{mn} = \sum_{m=0}^{N-1} \sum_{n=0}^{N-1} \alpha_p \alpha_q c_{pq} \cos \frac{\pi(2m+1)p}{2N} \cos \frac{\pi(2n+1)q}{2N} \end{cases} \quad (9)$$

$(0 \leq p, q, m, n < N)$

2-D DCT is closely related to the discrete Fourier transform. It is a separable linear transformation. That is, the result of 2-D DCT may be obtained by first taking transforms along the columns of F and then along the rows of that result [1, 2]. That is [1, 2],

$$C = DFD \quad (10)$$

In image compression, the input image is divided into 8-by-8 or 16-by-16 blocks, and the 2-D DCT is computed for each block. The DCT coefficients are then quantized, coded, and transmitted. The receiver decodes the quantized DCT coefficients, computes the inverse 2-D DCT of each block, and then puts the blocks back together into a single image.

Almost all of digital films such as VCD and digital pictures such as JPEG files are compressed by using DCT currently. Real-time compressing and high compression ratio are the main research topics of image compression [2]. The time complexity of classical 1-D DCT and 2-D DCT is $O(N \log_2 N)$ and $O(N^2 \log_2 N)$ respectively [1, 2]. The more N is big, the more the compression ratio is high if the whole input data sequence is Markov chain and the order of chain is bigger than N , but the running time increases drastically so that real-time compressing is impossible. That is, finding a fast algorithm for large N is significant.

3. Two Properties of DCT of Image

- **Property 1:** 2-DCT of image is an energy conservation transform [1, 2], i.e.,

$$\sum_{m=0}^{N-1} \sum_{n=0}^{N-1} (f_{mn})^2 = \sum_{p=0}^{N-1} \sum_{q=0}^{N-1} (c_{pq})^2$$

1-D DCT is same too.

The property is utilized as halt criterion of algorithm in this paper. If we find some DCT coefficients (e.g., c_{00}, c_{01}, c_{10}) such that $\sum_{m=0}^{N-1} \sum_{n=0}^{N-1} (f_{mn})^2 \approx (c_{00})^2 + (c_{01})^2 + (c_{10})^2$, we will halt algorithm. That is, c_{00}, c_{01}, c_{10} keep the information of image approximately.

- **Property 2:** For typical images, many of the DCT coefficients have values close to zero; these coefficients can be discarded without seriously affecting the quality of the reconstructed image [1, 2].

Fig. 2, Fig. 3 and Table 1 illustrate the property 2 [3]. The property is utilized to design quantum algorithm in this paper.

Fig2

Fig3

(suggested minification: 60%) (suggested minification: 60%)

Table 1

C. The Classical Parallel Circuit for Computing Inner Product

Notation 1 t_A denotes the running time of addition $a + b$ or subtraction $a - b$.

Notation 2 t_M denotes the running time of multiplication $a \times b$.

Notation 3 t_D denotes the running time of division $\frac{a}{b}$. In general, the time of division is little bigger than the time of multiplication.

Notation 4 t_C denotes the running time of comparison $a \leq b$ or $a \geq b$.

In classical computer, there exist constants m_1 and m_2 such that $t_M \geq m_1 t_A$ and $t_D \geq m_2 t_M$. The values of m_1 and m_2 relate with the material architecture of central processing unit (CPU). Different CPU has different values of m_1 and m_2 [4]. For the convenience of computation, without loss of generality, we suppose

$$t_M \geq 25t_A, t_M = 2t_D \text{ and } t_A \gg t_C$$

The assumption does not affect the time complexity because time complexity is only associated with the order of parameter N . E.g., $O(\frac{\pi}{4}\sqrt{N}) = O(\sqrt{N})$ and $O(\frac{\pi}{4}\sqrt{N}) \neq O(N)$.

Let $N - dimensional$ vector

$$\begin{aligned}\vec{x} &= (x_0, x_1, \dots, x_{N-1})^T \\ \vec{y} &= (y_0, y_1, \dots, y_{N-1})^T\end{aligned}$$

The inner product is defined as

$$\vec{x} \bullet \vec{y} = \sum_{k=0}^{N-1} x_k \times y_k$$

The classical parallel circuit for computing inner product can be designed easily. Fig. 4 illustrates a realization of the classical parallel circuit.

Insert Fig4 Here

Notation 5 t_I denotes the running time of parallel computation of inner product.

Clearly, $t_I = 1 \times t_M + \lceil \log_2 N \rceil t_A$
when $N \leq 2^{4 \times 25}$, $t_I \leq 1 \times t_M + 4 \times (25t_A) \leq 5t_M$
Because $N = 2^{100}$ is a very giant number, we regard t_I as

$$t_I \leq 5t_M \tag{11}$$

D. Introduction of Quantum Computation

Recent research shows that realizing image compression by using quantum computer is possible. For example, Pang recently presents a quantum algorithm to realize the encoding of Vector Quantization, which is very faster than classical encoding algorithm [5]. This paper presents a quantum algorithm to realize DCT for image compression.

1. Introduction of Quantum Bit (qubit)

Just as classical bit has state - either 0 or 1 - a qubit also has a state. Two possible states for a qubit are the states $|0\rangle$ and $|1\rangle$, which as you might guess correspond to the states 0 and 1 for a classical bit. Notation like $| \rangle$ is called the Dirac notation, and we'll be seeing it often, as it's the standard notation for states in quantum mechanics. The difference

between bits and qubit can be in a state *other* than $|0\rangle$ or $|1\rangle$. It is also possible to form linear combinations of states, often called superpositions

$$|\psi\rangle = \alpha|0\rangle + \beta|1\rangle$$

The numbers α and β are complex numbers. Put another way, the state of a qubit is a vector in a two-dimensional complex vector space. The special states $|0\rangle$ and $|1\rangle$ are known as computational basis states, and form an orthonormal basis for this vector space.

We can examine a bit to determine whether it is in the state 0 or 1 in classical computer. By contrast, when we measure a qubit, we get either the result 0, with probability $|\alpha|^2$, or the result 1, with probability $|\beta|^2$. Naturally, $|\alpha|^2 + |\beta|^2 = 1$. In general a qubit is a unit vector in a two-dimensional complex vector space [6].

We explain the superpositions $|\psi\rangle = \alpha|0\rangle + \beta|1\rangle$ by analogy with sonic wave as following.

Suppose there are three persons Alice, Bob and you in a closed room. Alice and Bob speak in a sample wave $|A\rangle = f_A(t) = e^{im\omega t}$ and $|B\rangle = f_B(t) = e^{in\omega t}$ respectively, where $m \neq n$ and they are both integers. We can distinguish Alice from Bob because the two sample waves are orthogonal (i.e., $\langle A|B\rangle = \int_0^{\frac{2\pi}{\omega}} e^{i(n-m)\omega t} dt = 0$). When Alice speak in the closed room, your ears will receive a sonic wave $g_A(t) = I_A e^{i\phi_A} |A\rangle$, where I_A is the amplitude of the wave and the phase ϕ_A is cause by the distance between Alice and you. If Alice and Bob speak simultaneously, your ears will receive a superposition:

$$|\psi_{AB}\rangle = I_A e^{i\phi_A} |A\rangle + I_B e^{i\phi_B} |B\rangle$$

Let

$$I = \sqrt{(I_A)^2 + (I_B)^2}$$

$$\alpha_A = \frac{I_A}{I} e^{i\phi_A} \text{ and } \beta_B = \frac{I_B}{I} e^{i\phi_B}$$

Thus,

$$|\psi_{AB}\rangle = I(\alpha_A |A\rangle + \beta_B |B\rangle)$$

Your ears can distinguish Alice's voice from the superposition $|\psi_{AB}\rangle$. That is, '+' implies two sonic wave $|A\rangle$ and $|B\rangle$ exist in the superposition simultaneously and they can be distinguished from the superposition. If Alice speaks very aloud (i.e., $|\alpha_A|^2 \rightarrow 1$ or $|\beta_B|^2 \rightarrow 0$), you will always hear Alice's voice. This case is analogous with the case $|\alpha|^2 \rightarrow 1$ of quantum computation. If $|\alpha|^2 \rightarrow 1$, you will get the result 0 always, with probability $|\alpha|^2 \approx 1$. This property is utilized to design quantum algorithm such as Grover's algorithm. You can operate the two distinguished sample wave $|A\rangle$ and $|B\rangle$ simultaneously. For example, you can send the voice $|\psi_{AB}\rangle$ in a radio and change Alice's volumes and Bob's volumes simultaneously by pushing the volume button on radio. That is, performing once operation causes the changing of two sonic waves simultaneously. This case is analogous with quantum parallelism. Fig. 5 shows the analogies between quantum superpositions and sonic wave.

Insert Fig5 Here

2. Operation of Computation Acting on Qubits

Classical computer circuits consist of wires and logic gates. The wires are used to carry information around the circuit, while the logic gates perform manipulations of the information, converting it from one form to another. It is the fundamental of classical computation

that classical computer circuits can realize the operations of Boolean algebra. For example, classical NOT gate makes 0 and 1 states interchanged. The operations of Boolean algebra can also be realized on quantum computer by utilizing single qubit gates and controlled-NOT gates. For example, quantum NOT gate takes the state $|\psi\rangle = \alpha|0\rangle + \beta|1\rangle$ to the corresponding state in which the role of $|0\rangle$ and $|1\rangle$ have interchanged. All digital operation can be realized by utilizing unitary operation that is the combination of some single qubit gates and controlled-NOT gates [6].

3. Quantum Parallelism

Quantum parallelism allows quantum computers to evaluate a function $f(x)$ for many different values of x simultaneously. The power of quantum computation is due to the fact that the state of a quantum computer can be a superposition of basis states and we can perform an operation on multiple quantum states simultaneously. For example, suppose $f(x) : \{0, 1\} \rightarrow \{0, 1\}$ is a function with a one-bit domain and range. We need at least two times calculating for obtain the values $f(0)$ and $f(1)$ on classical computer. For arbitrary function $f(x)$, there is quantum circuit U_f that can transform $|0, y\rangle$ and $|1, y\rangle$ into $|0, y \oplus f(0)\rangle$ and $|1, y \oplus f(1)\rangle$ respectively by performing only one time calculating, where \oplus indicates addition modulo 2. That is, $\frac{|0\rangle|y\rangle + |1\rangle|y\rangle}{\sqrt{2}} \xrightarrow{U_f} \frac{|0\rangle|y \oplus f(0)\rangle + |1\rangle|y \oplus f(1)\rangle}{\sqrt{2}}$, where '+' implies two states $|0\rangle|y\rangle$ and $|1\rangle|y\rangle$ exist in the superposition of states simultaneously. The formula implies also that the two states $|0\rangle|y\rangle$ and $|1\rangle|y\rangle$ are converted to $|0\rangle|y \oplus f(0)\rangle$ and $|1\rangle|y \oplus f(1)\rangle$ simultaneously. That is, the values $f(0)$ and $f(1)$ are calculated simultaneously [6, 7].

4. Introduction of quantum Fourier transform (QFT), Klappenecker's DCT and Latorre's Quantum Representation of Image

The quantum Fourier transform (QFT [6, 7]) on an orthonormal basis $|0\rangle, |1\rangle, \dots, |N-1\rangle$ is defined to be a linear operator with the following action on the basis states,

$$QFT|j\rangle = \frac{1}{\sqrt{N}} \sum_{k=0}^{N-1} e^{2\pi i j k / N} |k\rangle$$

Equivalently, the action on an arbitrary state may be written

$$QFT\left(\sum_{j=0}^{N-1} \alpha_j |j\rangle\right) = \sum_{j=0}^{N-1} \alpha_j (QFT|j\rangle)$$

Similar to other unitary operation, QFT is unitary operation that only acts on basis states. It's an error opinion that unitary operation can act on coefficients of basis states. Figure 6 illustrates that QFT only acts on basis states $|0\rangle$ and $|1\rangle$.

Insert Fig6 Here

Klappenecker presents a method to realize DCT of types I, II, III, and IV on a quantum computer by utilizing QFT [8]. Define DCT of types I as [8]

$$C_N^I := \sqrt{\left(\frac{2}{N}\right)} [\alpha_i \cos \frac{ij\pi}{N}]_{i,j=0\dots N}$$

The discrete sine transforms (DST) of types I denoted by S_N^I is defined accordingly. [8]
Let discrete Fourier transform (DFT) be [8]

$$F_N = \frac{1}{\sqrt{N}} \left[\sum_{k=0}^{N-1} (e^{2\pi ijk/N}) \right]_{k,l=0\dots N-1}$$

Let [8]

$$T_N = \begin{pmatrix} 1 & & & & & \\ & \frac{1}{\sqrt{2}} & & & & \\ & & \ddots & & & \\ & & & \frac{1}{\sqrt{2}} & & \\ & & & & 1 & \\ & & & & & \frac{1}{\sqrt{2}} \\ & & & & & & -\frac{i}{\sqrt{2}} \\ & & & & & \ddots & \\ & \frac{1}{\sqrt{2}} & & & & & & -\frac{i}{\sqrt{2}} \end{pmatrix}$$

Klappenecker's DCT derives from QFT and depends on QFT. Indeed, the DST and DCT can be recovered from the DFT by a base change

$$T_N^+ \cdot F_{2N} \cdot T_N = C_N^I \oplus iS_N^I$$

Since efficient quantum circuit for the DFT (i.e., QFT) are known, it remains to find an efficient implementation of the matrix T_N . A quantum circuit is proposed by Klappenecker to realize the matrix T_N . This is the primitive idea of Klappenecker's DCT [8].

The result of QFT or Klappenecker's DCT seems to indicate that quantum computer can be used to very quickly compute the Fourier transform, which would be fantastically useful in a wide range of applications. However, that is *not* exactly the case; the Fourier transform or Klappenecker's DCT is being performed on the information 'hidden' in the amplitudes of the quantum state. This information is not directly accessible to measurement. The catch, of course, is that if the output state is measured, it will collapse each qubit into the state $|0\rangle$ or $|1\rangle$, preventing us from learning the transform result directly[6]. In addition, the contents of section 2.1 in this paper shows that Klappenecker's DCT cannot be applied to DCT of image compression too. Klappenecker's DCT is useful on many other signal processing maybe.

Latorre presentes a novel quantum representation for image compression [19]. The entropy of images is, in general, very large. An image with large entropy is hard to compress. The idea in Latorre's paper is to keep the largest eigenvalues of the Schmidt decompositions when the picture is written in a renormalization group manner, that is, the largest contribution to the entropy in that basis. Latorre's algorithm is nice but it is not competitive with jpeg. The reason is that jpeg uses details of how human see. The quantization table used in jpeg is tailored to the human eye. Unless there are quantum quantization methods are incorporated in Latorre's algorithm, there is no way it is as efficient as jpeg.

E. Introduction of Grover's Algorithm and Boyer's Algorithm

The algorithm by Grover solves the problem of searching for an element with a unique index x_0 in a list of N unsorted elements, similar to searching a database like a telephone directory when we know the number but not the person's name [7]. Grover's quantum searching algorithm [9] takes advantage of quantum mechanical properties to perform the search with an efficiency of order $O(\sqrt{N})$ [6].

To implement the quantum search we need to construct a unitary operation that discriminates between the marked item x_0 and the rest. The following function,

$$f(x) = \begin{cases} 0 & \text{if } x \neq x_0 \\ 1 & \text{if } x = x_0 \end{cases}$$

and its corresponding unitary operation (i.e., black box or oracle),

$$O|x\rangle = (-1)^{f(x)}|x\rangle$$

will do the job.

The Grover iteration is defined as [5]

$$G = (2|\Psi\rangle\langle\Psi| - I)O \tag{12}$$

on $N - dimensional$ Hilbert space, where $|\Psi\rangle = \frac{1}{\sqrt{N}} \sum_{x=0}^{N-1} |x\rangle$.

The Grover iteration can be regarded as a rotation in the two-dimensional space spanned by $|\Psi\rangle$ and $|x_0\rangle$. To see this it is useful to let $|\alpha\rangle = \frac{1}{\sqrt{N-1}} \sum_{x \neq x_0} |x\rangle$ indicate a sum over all x which are not solutions to the search problem. Thus,

$$|\Psi\rangle = \sqrt{\frac{N-1}{N}}|\alpha\rangle + \sqrt{\frac{1}{N}}|x_0\rangle$$

so the initial state of the quantum computer is in the space spanned by $|x_0\rangle$ and $|\alpha\rangle$. Let

$$\sin \theta/2 = \sqrt{1/N}$$

As Figure 7 shows, G is a rotation in the two-dimensional space $span\{|x_0\rangle, |\alpha\rangle\}$, rotating the state $|\Psi\rangle$ by θ radians per application of G . Repeated application of the Grover iteration rotates the state vector close to $|x_0\rangle$. When this occurs, an observation in the computational basis produces with high probability [6]. This is the key of Grover's algorithm.

Insert Fig7 Here

Eli Biham's papers show that Grover's algorithm is suitable for the case of an arbitrary initial amplitude distribution [10, 11]. Gui-Lu Long improves Grover's algorithm to 100% successful probability even the number is very small [12, 13].

Michel Boyer, et., al. present the following algorithm for the case that the number of solutions t is unknown [14].

Algorithm 6 *Boyer's algorithm*

1. Initialize $m = 1$ and set $\lambda = 6/5$.
(Any value of λ strictly between 1 and 4/3 would do.)
2. Choose j uniformly at random among the nonnegative integers smaller than m .
3. Apply j iterations of Grover's algorithm starting from initial state $|\psi_0\rangle = \sum_i \frac{1}{\sqrt{N}}|i\rangle$
4. Observe the register: let i be the outcome.
5. If $T[i] = x$, the problem is solved: exit.
6. Otherwise, set m to $\min(\lambda m, \sqrt{N})$ and go back to step 2.

Boyer's algorithm is derived from Grover's algorithm and has time complexity $O(\sqrt{\frac{N}{t}})$. The case of $t = 0$ is handled by it. It is a very smart algorithm because it saves many quantum circuits comparing with the other algorithms by using quantum counting technique that will need exponential order circuits [6]. Boyer's algorithm is utilized in this paper. The one of the tasks of this paper is to design appropriate quantum iteration (named quantum DCT iteration in this paper) according to DCT properties to substitute for the Grover iteration in Boyer's algorithm.

In this paper, Each ket represents a register rather than a single qubit. In this paper, similar to other quantum algorithm [6, 7], ancilla qubits are ignored.

II. THE REPRESENTATION OF IMAGE BY USING QUANTUM STATES

A. Classical Data Structure of 1-D DCT

For a given vector $x = (x_0, x_1, \dots, x_{N-1})$, we can declare a BYTE array "BYTE $x[N]$ " to store it by using c language, where c language is compiler language of classical computer [15]:

$$x[0] = x_0, x[1] = x_1, \dots, x[N - 1] = x_{N-1}$$

There is a logical mapping to associate subscript with component of vector x :

$$\begin{aligned} \text{Mapping} : i &\longmapsto x[i] \\ (0 \leq i < N) \end{aligned} \tag{13}$$

The logical mapping is necessary because it associates data with the corresponding logical address. CPU accesses value $x[i]$ according to the subscript i (i.e., logical address).

The mapping is done by memory-management unit (MMU) of Operating System [16]. The operation of accessing data is a very very fast operation so that the time of access can be ignored when designing algorithm.

Fig8 illustrates the logical mapping. Fig9 illustrates the physical realization of the logical mapping [16].

Insert Fig8 Here

Insert Fig9 Here

Similar to vector x , the vectors \vec{f}_i (equation 2), \vec{c} (equation 8), \vec{D}_u (equation 6), matrix D (equation 7) and matrix F (equation 1) can be stored in array respectively, and the Operating System of classical computer will establish the mapping (equation 13) automatically [16].

For example, we declared a two dimensional array " *BYTE arrayImage[N][N]*" to store matrix F . The mapping between position (i, j) and pixel value f_{ij} is defined as

$$Mapping : (i, j) \mapsto arrayImage[i][j] = f_{ij} \quad (14)$$

The above mapping (equations 13 and 14) should be also kept in quantum computation so that arbitrary component of vector or matrix is associated with the corresponding subscript.

By the definition of DCT (equations (4) and (9)), *QFT* and Klappenecker's DCT cannot both keep the mapping. Therefore, More suitable quantum data structure is required in order to keep the mapping and harness the power of quantum computation for image compression.

B. The Quantum Representation of Image

1. Data Structure of Quantum Representation of Image

To keep the mapping in equations (13) and (14), the following database technique is presented to represent image F (equation (1)) in this paper:

First, all vectors $\vec{f}_i = (f_{0i}, f_{1i}, \dots, f_{(N-1)i})^T$ ($0 \leq i < N$) are stored in a database. Each vector is regard as a record with unique index i .

Second, all vectors are loaded into CPU simultaneously and form the superposition of states $\frac{1}{\sqrt{N}}|ancilla1\rangle(\sum_{i=0}^{N-1}|i\rangle|\vec{f}_i\rangle)|ancilla2\rangle$ by using quantum addressing scheme and unitary operation LOAD.

LOAD operation that is denoted by U_L is defined as

$$|i\rangle|0\rangle \cdots |0\rangle \xrightarrow{U_L} |i\rangle|0 \oplus f_{0i}\rangle \cdots |0 \oplus f_{(N-1)i}\rangle$$

, where \oplus denotes addition modulo 2, that can be realized by utilizing controlled NOT operation [6].

In vector notation,

$$|i\rangle|0\rangle \xrightarrow{U_L} |i\rangle|0 \oplus \vec{f}_i\rangle \quad (15)$$

LOAD operation is the basic operation of quantum computer ([6], chapter 6).

Figure 10 illustrates the representation of image by using quantum states.

Insert Fig10 Here

The proposed representation of image in this paper keep the mapping in equation (14) so that subscript (j, i) is associated with corresponding pixel value f_{ji} . State $\frac{1}{\sqrt{N}}|ancilla1\rangle(\sum_{i=0}^{N-1}|i\rangle|\vec{f}_i\rangle)|ancilla2\rangle$ is entanglement state when *ancilla1* and *ancilla2* are constants. Therefore, if we obtain value i from the second register, we will get the unique mapping vector \vec{f}_i in third register. Thus, the mapping is kept.

2. The Time of Load Operation U_L

Notation 7 t_L denotes the time of performing one time operation $|i\rangle|0\rangle \mapsto |i\rangle|0 \oplus f_{ji}\rangle$, where f_{ji} is a component of vector \vec{f}_i .

Notation 8 $Time(U)$ denotes the time of performing one time operation U .

The time of LOAD operation U_L in equation (15) is denoted by $Time(U_L)$.

The time of data access (i.e., loading data into registers from memory) is ignored in classical algorithm when design algorithm. It is clear that the most efficient possible algorithm is in this model of computation ([6], chapter 6, section 6.5 or [16]). Operation $|i\rangle|0\rangle \mapsto |i\rangle|0 \oplus f_{ji}\rangle$ is CNOT operation, and it is a very very fast operation so that it's running time can be ignored when analyze the time complexity of algorithm ([6], chapter 6). Because each component f_{ji} is saved in memory independently, each component can be load into register simultaneously by utilizing parallel circuit in classical case. Furthermore, the classical circuit can be translated into a quantum reversible circuit. [6] Therefore, in general,

$$Time(U_L) = t_L \approx 0 \quad (16)$$

III. QUANTUM 1-D DCT ITERATION

A. The Design of Oracle O_{inner} , O'_{inner} and O_f

All of vectors \vec{D}_i in equations (5) and (6) are stored in a database (Fig10). Each vector \vec{D}_i has a unique index i , where $0 \leq i < N$.

An arbitrary vectors \vec{D}_i is loaded into registers according to the corresponding index i by using unitary operation U_L (Fig10):

$$|\alpha\rangle|\beta\rangle|i\rangle|\vec{f}\rangle|0\rangle|0\rangle|0\rangle \xrightarrow{U_L} |\alpha\rangle|\beta\rangle|i\rangle|\vec{f}\rangle|\vec{D}_i\rangle|0\rangle|0\rangle \quad (17)$$

where α and β is two input parameters.

1. Oracle O_{inner} and O'_{inner}

It's easy to construct a classical parallel circuit to calculate inner product (Section I-C and Fig. 4). Furthermore, the classical circuit can be translated into a quantum reversible circuit [6], that has the same time complexity with it's corresponding classical circuit.

We design oracles O_{inner} and O'_{inner} to compute the inner product between two vectors \vec{D}_i and \vec{f} .

$$|\alpha\rangle|\beta\rangle|i\rangle|\vec{f}\rangle|\vec{D}_i\rangle|0\rangle|0\rangle \xrightarrow{O_{inner}} |\alpha\rangle|\beta\rangle|i\rangle|\vec{f}\rangle|\vec{D}_i\rangle|0\rangle|(\vec{D}_i \bullet \vec{f})^2\rangle \quad (18)$$

$$|\alpha\rangle|\beta\rangle|i\rangle|\vec{f}\rangle|\vec{D}_i\rangle|0\rangle|0\rangle \xrightarrow{O'_{inner}} |\alpha\rangle|\beta\rangle|i\rangle|\vec{f}\rangle|\vec{D}_i\rangle|\vec{D}_i \bullet \vec{f}\rangle|0\rangle \quad (19)$$

Figure 11 illustrates the oracles O_{inner} .

Insert Fig11 Here

By equation (11), oracles O_{inner} has time complexity

$$Time(O_{inner}) = t_I + 1 \times t_M \leq 6t_M \quad (20)$$

Oracles O'_{inner} has time complexity

$$Time(O'_{inner}) = t_I \leq 5t_M \quad (21)$$

2. Oracle O_f

Define a function f as following

$$f(i) = \begin{cases} 1 & \text{if } \alpha \leq (\vec{D}_i \bullet \vec{f})^2 \leq \beta \\ 0 & \text{otherwise} \end{cases}$$

We design other oracle denoted by O_f that is used to mark the retained DCT coefficients (Table 1):

$$|\alpha\rangle|\beta\rangle|i\rangle|\vec{f}\rangle|\vec{D}_i\rangle|0\rangle|(\vec{D}_i \bullet \vec{f})^2\rangle \xrightarrow{O_f} (-1)^{f(i)}|\alpha\rangle|\beta\rangle|i\rangle|\vec{f}\rangle|\vec{D}_i\rangle|0\rangle|(\vec{D}_i \bullet \vec{f})^2\rangle \quad (22)$$

Figure 12 illustrates the oracles O_f .

Insert Fig12 Here

Oracle O_f has time complexity .

$$Time(O_f) = 2t_C \quad (23)$$

B. Quantum 1-D DCT Iteration G_{DCT}

Let $(O_{inner})^{-1}$ denote the inverse transform of O_{inner} .

Let $(U_L)^{-1}$ denote the inverse transform of U_L .

$$(O_{inner}U_L)^{-1} = (U_L)^{-1}(O_{inner})^{-1}$$

Definition 9 By equations (17), (18) and (22), quantum 1-D DCT iteration G_{DCT} is defined as

$$G_{DCT} = (2|\xi\rangle\langle\xi| - I)(U_L)^{-1}(O_{inner})^{-1}O_fO_{inner}U_L \quad (24)$$

, where $|\xi\rangle = \frac{1}{\sqrt{N}} \sum_{i=0}^{N-1} |i\rangle$.

We have

$$(U_L)^{-1}(O_{inner})^{-1}O_fO_{inner}U_L|\alpha\rangle|\beta\rangle|i\rangle|\vec{f}\rangle|0\rangle|0\rangle|0\rangle = (-1)^{f(i)}|\alpha\rangle|\beta\rangle|i\rangle|\vec{f}\rangle|0\rangle|0\rangle|0\rangle \quad (25)$$

Equation (25) shows that the state $|\alpha\rangle|\beta\rangle|i\rangle|\vec{f}\rangle|0\rangle|0\rangle|0\rangle$ is the eigenstate of unitary operation $(U_L)^{-1}(O_{inner})^{-1}O_fO_{inner}U_L$ and the eigenvalue is $(-1)^{f(i)}$. This is a key of applying two or more oracles to perform complex search.

Figure 13 shows the action of unitary $(U_L)^{-1}(O_{inner})^{-1}O_fO_{inner}U_L$.

Insert Fig13 Here

Let $\text{span}\{|i\rangle \otimes |\text{vector}\rangle \otimes |\text{innerproduct}\rangle\}$ be the global space that spanned by $|i\rangle$, N – dimensional vector $|\text{vector}\rangle$, and the value of inner product $|\text{innerproduct}\rangle$.

Let $\text{span}\{|i\rangle \mid 0 \leq i < N\}$ be the subspace that is the span of all states $|i\rangle$.

Theorem 10 (Figure 14, 15) G_{DCT} is a rotation on N – dimensional subspace $\text{span}\{|i\rangle \mid 0 \leq i < N\}$. For initial state $|\psi_0\rangle = \frac{1}{\sqrt{N}} \sum_{i=0}^{N-1} (|\alpha\rangle|\beta\rangle|i\rangle|\vec{f}\rangle|0\rangle|0\rangle|0\rangle)$, the rotation angle is $\theta = 2 \arcsin \sqrt{\frac{t}{N}}$, where t is the number of solutions.

Proof 11 For arbitrary input state

$$|\text{input}\rangle = \sum_{i=0}^{N-1} A_i (|\alpha\rangle|\beta\rangle|i\rangle|\vec{f}\rangle|0\rangle|0\rangle|0\rangle)$$

where A_i is the probability amplitude of the state and

$$\sum_{i=0}^{N-1} |A_i|^2 = 1$$

By equation (25), we have

$$G_{DCT}|\text{input}\rangle = |\alpha\rangle|\beta\rangle$$

$$\underbrace{\{(2|\xi\rangle\langle\xi| - I) \left(\sum_{i=0}^{N-1} (-1)^{f(i)} A_i |i\rangle \right)\}}_{|\vec{f}\rangle|0\rangle|0\rangle|0\rangle} \quad (26)$$

Equation (26) shows that unitary operation $2|\xi\rangle\langle\xi| - I$ only acts on state $\sum_{i=0}^{N-1} (-1)^{f(i)} A_i |i\rangle$.

Suppose that the solutions set is

$$S = \{|\alpha\rangle|\beta\rangle|i\rangle|\vec{f}\rangle|0\rangle|0\rangle|0\rangle \mid \alpha \leq (\vec{D}_i \bullet \vec{f})^2 \leq \beta\}$$

All solutions form a superposition

$$|\tau\rangle = \frac{1}{\sqrt{|S|}} \sum_{|u\rangle \in S} |u\rangle = \frac{1}{\sqrt{|S|}} |\alpha\rangle |\beta\rangle \underbrace{\left(\sum_S |i\rangle \right) |\vec{f}\rangle |0\rangle |0\rangle |0\rangle}$$

Let

$$|\sigma\rangle = \frac{1}{\sqrt{N - |S|}} \sum_{|v\rangle \notin S} |v\rangle = \frac{1}{\sqrt{N - |S|}} |\alpha\rangle |\beta\rangle \underbrace{\left(\sum_{I-S} |j\rangle \right) |\vec{f}\rangle |0\rangle |0\rangle |0\rangle}$$

The initial state $|\psi_0\rangle$ is rotated in the subspace $\text{span}\{|\sigma\rangle, |\tau\rangle\}$ by θ towards the superposition $|\tau\rangle$ of all solutions to the search.

Initially, it is inclined at angle $\frac{\theta}{2}$ from $|\sigma\rangle$, a state orthogonal to $|\tau\rangle$.

By equation (25), the product operation $(U_L)^{-1}(O_{inner})^{-1}O_f O_{inner}U_L$ reflects the state about the state $|\sigma\rangle$. Then the operation $2|\xi\rangle\langle\xi| - I$ reflect it about $|\xi\rangle$.

Notice that $|\tau\rangle \in \text{span}\{|i\rangle\}$ and $|\sigma\rangle \in \text{span}\{|i\rangle\}$.

Therefore, similar to Grover's iteration, the quantum 1-D DCT iteration G_{DCT} is a rotation on subspace $\text{span}\{|i\rangle\}$, and the rotation angle is $\theta = 2 \arcsin \sqrt{\frac{t}{N}}$.

Fig14 illustrates the action of a single G_{DCT} .

Fig15 shows that G_{DCT} is equivalent to a rotation on subspace $\text{span}\{|i\rangle\}$.

Insert Fig14 Here

Insert Fig15 Here

1-D DCT iteration G_{DCT} has time complexity

$$\text{Time}(G_{DCT}) = 2\text{Time}(U_L) + 2\text{Time}(O_{inner}) + \text{Time}(O_f)$$

By equations (16), (20) and (23), when $N \leq 2^{100}$,

$$\text{Time}(G_{DCT}) \leq 2t_C + 12t_M$$

Because $t_M \geq 25t_A \gg t_C$, we have

$$\text{Time}(G_{DCT}) \leq 13t_M \tag{27}$$

The theorem shows that the quantum 1-D DCT iteration G_{DCT} and the Grover iteration $G = (2|\Psi\rangle\langle\Psi| - I)O$ have the same property that they are both a rotation on space. However, comparing with Grover iteration that has only one oracle, G_{DCT} comprises two oracles O_{inner} and O_f so that it can perform complex search. Equation (25) is a key of applying two or more oracles to perform complex search. If there is no equation (25), applying two or more oracles is no significant.

IV. QUANTUM 1-D DCT OF IMAGE COMPRESSION

A. Subroutine 1: Finding a DCT Coefficient $c_{i_0} \in \{c_i \mid \alpha \leq (c_i)^2 \leq \beta\}$

Subroutine 1 is similar to Boyer's algorithm, and the Grover iteration in Boyer's algorithm is substituted by the iteration G_{DCT} .

Algorithm 12 *Subroutine 1*

Input parameters: α, β

Outputs: subscript i_0 and coefficient c_{i_0} ; a global Boolean variable $IsSolution$.

Step1. Initialize $m = 1$ and $\lambda = \frac{6}{5}$; $IsSolution = FALSE$;

Step2. Choose j uniformly at random among the nonnegative integers not bigger than m .

Step3. Generate the initial state

$$|\Psi_0\rangle = \frac{1}{\sqrt{N}}|\alpha\rangle|\beta\rangle \left(\underbrace{\sum_{i=0}^{N-1} |i\rangle}_{\vec{f}} \right) |0\rangle|0\rangle|0\rangle$$

This can be achieved in $O(\log_2 N)$ steps using a $\lceil \log_2 N \rceil$ - bit Hadamard transformation.

Step4. Apply j iterations of G_{DCT} starting from the state $|\Psi_0\rangle$. i.e.,

$$|\Psi_j\rangle = (G_{DCT})^j |\Psi_0\rangle$$

Step5. Perform computation .

$$|\Psi_{end}\rangle = O'_{inner} U_L |\Psi_j\rangle$$

Step6. Observe the third and the fifth register: let i_0, c_{i_0} be the outcome respectively.

Step7. If $c_{i_0} \in \{c_i \mid \alpha \leq (c_i)^2 \leq \beta\}$, Let $IsSolution = TRUE$, and *exit*; otherwise, go to step 8.

Step8. set m to $\min\{\lambda m, \sqrt{N}\}$ and go to step 2.

Figure 16 shows the processing of subroutine 1.

Insert Fig16 Here (suggested minification: 78%)

B. The Correctness of Subroutine 1

When $2^8 \leq N \leq 2^{100}$, $|\frac{\sin(\frac{1}{\sqrt{N}})}{\frac{1}{\sqrt{N}}} - 1| \leq 6.5 \times 10^{-4}$, $99.6\% \leq 1 - \frac{1}{N} < 1$. That is, when $2^8 \leq N \leq 2^{100}$, Grover's algorithm is still an efficient possible algorithm and the success probability $p = 1 - o(\frac{1}{N}) \geq 99.6\%$ [6]. Long improves Grover's algorithm so that the improved algorithm with 100% success probability even N is very small [12, 13].

The theorem in this paper demonstrates that G_{DCT} is similar to the Grover iteration. Therefore, subroutine 1 is correct.

C. The Time Complexity of Subroutine 1

Let κ presents the iteration steps of applying G_{DCT} .
Subroutine 1 has time complexity

$$Time(subroutine1) \leq \kappa[Time(G_{DCT}) + Time(O'_{inner}) + \lceil \log_2 N \rceil Time(Hadamard) + 2t_m + 3t_c]$$

, where $Time(Hadamard)$ represents the time of Hadamard transform acting on a single qubit.

when $N \leq 2^{100}$, we have

$$\log_2 N Time(Hadamard) \approx 0$$

Because $t_M \geq 25t_A \gg t_C$, by equations (21) and (27)

$$Time(subroutine1) \leq 21\kappa t_M$$

Subroutine 1 is similar to Boyer's algorithm. Hence

$$\kappa = O\left(\sqrt{\frac{N}{t}}\right)$$

Therefore,

$$Time(subroutine1) = O\left(\sqrt{\frac{N}{t}}\right)t_M \quad (28)$$

D. Quantum 1-D DCT of Image Compression

Algorithm 13 Quantum 1-D DCT of Image Compression (QDCT1)

Input: $\{\vec{D}_i | 0 \leq i < N\}$: The line vectors of DCT matrix (equation 5, 6, and 7). These line vectors are stored in database with indices i (Fig10);

Vector \vec{f} (equation 2)

Parameters: ΔE , α , β , threshold value $\varepsilon > 0$;

$nCount_i$ ($0 \leq i < N$): Counting the repeated times of coefficient c_i that is found when repeatedly applying subroutine 1.

$nMaxRepetition$: The maximum number of allowed repeated times of applying subroutine 1.

nS : The number of solutions that have been obtained.

Output: The big DCT coefficients and corresponding indices (i_0, c_{i_0}) , (i_1, c_{i_1}) , \dots , (i_R, c_{i_R}) such that $\frac{\sum_{k=0}^R (c_{i_k} \times c_{i_k})}{\|\vec{f}\|^2} \leq \varepsilon$, where $\|\vec{f}\|^2 = (\vec{f} \bullet \vec{f}) = \sum_{i=0}^{N-1} (f_i \times f_i)$. The other coefficients are set to zero (Table 1).

Step 0 (Initialize parameters): $\Delta E = \|\vec{f}\|^2$, $\alpha = \frac{\Delta E}{N}$, $\beta = \Delta E$; $nS = 0$; $nCount_i = 0$, where $0 \leq i < N$.

The proposed parallel circuit in section I-C (figure 4) can be applied to calculate the value $\|\vec{f}\|^2 = (\vec{f} \bullet \vec{f})$.

while($\frac{\Delta E}{\|\vec{f}\|^2} \geq \varepsilon$)
{
Step 1: Apply subroutine 1 to find a coefficient (i_k, c_{i_k}) ;
Step 2: If $IsSolution = TRUE$ and $nCount_{i_k} = 0$,
then $\Delta E = \Delta E - c_{i_k} \times c_{i_k}$; $nS = nS + 1$; $\alpha = \frac{\Delta E}{N-nS}$, $\beta = \Delta E$; $nCount_{i_k} = nCount_{i_k} + 1$;
If $IsSolution = TRUE$ and $0 < nCount_{i_k} < nMaxRepetition$, continue;
If $IsSolution = TRUE$, and $nCount_{i_k} \geq nMaxRepetition$, **exit** and apply classical algorithm to obtain DCT coefficients;
If $IsSolution = FALSE$, **exit** and apply classical algorithm to obtain DCT coefficients;
}

Example 14 We choose the first 8 number gray value of the first line of image in fig. 2 as vector \vec{f} . That is,

$$\vec{f} = (f_{00}, f_{01}, f_{02}, \dots, f_{07})^T = (156, 159, 158, 155, 158, 156, 159, 158)^T$$

$$c = (c_0, c_1, c_2, \dots, c_7) = DCT(\vec{f})$$

$$((c_0)^2, (c_1)^2, (c_2)^2, \dots, (c_7)^2) = (1.9814e + 005, 0.51531, 1.5063, 0.95824, 3.125, 2.5846, 2.7437, 4.4418)^T$$

Let $\varepsilon = 2.0 \times 10^{-5}$

The computation procedure of 1-D QDCT is listed below:

Step A (Fig17). **Input:** $\Delta E = \|\vec{f}\|^2 = 198151$, $\beta = \Delta E$, $\alpha = \frac{\Delta E}{8} = 24768.875$;

Output: The set of solutions $S = \{(k, c_k) \mid \alpha \leq (c_k)^2 \leq \beta\} = \{(0, c_0)\}$. The output is the unique solution $(0, c_0)$.

Insert Fig17 Here

Step B (Fig18). **Input:** $\Delta E = \Delta E - (c_0)^2 = 11$, $\frac{\Delta E}{\|\vec{f}\|^2} = 5.55132 \times 10^{-5}$, $\beta = \Delta E$, $\alpha = \frac{\Delta E}{8-1} = 1.57143$;

Output: The set of solutions $S = \{(4, c_4), (5, c_5), (6, c_6), (7, c_7)\}$.

We will obtain one of solution with equal probability. Suppose the output is $(6, c_6)$.

Insert Fig18 Here

Step C. Input: $\Delta E = \Delta E - (c_6)^2 = 8.2563$, $\frac{\Delta E}{\|\vec{f}\|^2} = 4.16667 \times 10^{-5}$, $\beta = \Delta E$, $\alpha = \frac{\Delta E}{8-2} = 1.37605$;

Output: The set of solutions $S = \{(2, c_2), (4, c_4), (5, c_5), (7, c_7), (6, c_6)\}$.

We will obtain a new solution with probability $p = \frac{4}{5}$. That is, repeating subroutine 1 $\lceil \frac{1}{p} \rceil$ times approximately, we will obtain a new solution. Suppose the output is $(7, c_7)$.

Because $\frac{\Delta E - (c_7)^2}{\|f\|^2} = 1.92505 \times 10^{-5} < \varepsilon$, stop.

E. Time Complexity of Quantum 1-D DCT of Image Compression (QDCT1)

Suppose the number of retained DCT coefficients is M .

For typical images, many of the DCT coefficients have values close to zero; these coefficients can be discarded without seriously affecting the quality of the reconstructed image [3] (section I-B.3., Table 1).

The above example shows that the only one retained DCT coefficient is c_0 if $\varepsilon = 5.56 \times 10^{-5}$. That is, c_0 keeps almost information of vector \vec{f} . Thus, $M = 1$ (i.e., $M \ll N$)

By equation (11), the step0 has complexity

$$Time(Step0) = t_I + t_D \leq 7t_M$$

The step1 has complexity

$$Time(Step1) = Time(subroutine1)$$

The step2 has complexity

$$Time(Step2) = t_M + t_D + 3t_A + 8t_C \leq 5t_M$$

Thus, the time complexity of QDCT1 is

$$\begin{aligned} Time(QDCT1) &= Time(Step0) + \\ &M(t_D + Time(Step1) + Time(Step2)) \\ &\leq 7t_M + M(7t_M + Time(subroutine1)) \end{aligned}$$

Because $M \ll N$, by equation (28), we have

$$Time(QDCT1) = O(\sqrt{N})t_M \quad (29)$$

V. QUANTUM 2-D DCT

By formula (10), the 2-D DCT can be expressed as

$$C = DFD = (DF)D = GD \quad (30)$$

,where

$$\begin{aligned} G &= DF = (g_{ij})_{N \times N} = (\vec{D}_i \bullet \vec{f}_j)_{N \times N} = \\ &= \begin{pmatrix} \vec{D}_0 \\ \vec{D}_1 \\ \vdots \\ \vec{D}_{N-1} \end{pmatrix} \begin{pmatrix} \vec{f}_0 & \vec{f}_1 & \dots & \vec{f}_{N-1} \end{pmatrix} \end{aligned} \quad (31)$$

A. The Data Structure of Computing Matrix G

2-D DCT is closely related to the discrete Fourier transform. It is a separable linear transformation, that is, the result of 2-D DCT may be obtained by first taking transforms along the columns of F and then along the rows of that result [1, 2].

Clearly, G is the result of 1-D DCT by taking transforms along the columns of F .

All of vectors \vec{D}_i and \vec{f}_j are stored in two different tables of database, where $0 \leq i, j < N$.

An arbitrary record \vec{D}_i or \vec{f}_j can be fetched into registers of CPU according to indices i, j by performing load operation U'_L .

Load operation U'_L is defined as

$$|\alpha\rangle|\beta\rangle \underbrace{|i\rangle|j\rangle}|0\rangle|0\rangle|0\rangle|0\rangle \xrightarrow{U'_L} |\alpha\rangle|\beta\rangle \underbrace{|i\rangle|j\rangle}|\vec{f}_j\rangle|\vec{D}_i\rangle|0\rangle|0\rangle \quad (32)$$

We design oracles B_{inner} and B'_{inner} to compute the inner product between two vectors \vec{D}_i and \vec{f}_j

$$|\alpha\rangle|\beta\rangle|i\rangle|j\rangle|\vec{f}_j\rangle|\vec{D}_i\rangle|0\rangle|0\rangle \xrightarrow{B_{inner}} |\alpha\rangle|\beta\rangle|i\rangle|j\rangle|\vec{f}_j\rangle|\vec{D}_i\rangle|0\rangle|(\vec{D}_i \bullet \vec{f}_j)^2\rangle \quad (33)$$

$$|\alpha\rangle|\beta\rangle|i\rangle|j\rangle|\vec{f}_j\rangle|\vec{D}_i\rangle|0\rangle|0\rangle \xrightarrow{B'_{inner}} |\alpha\rangle|\beta\rangle|i\rangle|j\rangle|\vec{f}_j\rangle|\vec{D}_i\rangle|(\vec{D}_i \bullet \vec{f}_j)\rangle|0\rangle$$

Define a function f' as following

$$f'(i, j) = \begin{cases} 1 & \text{if } \alpha \leq (\vec{D}_i \bullet \vec{f}_j)^2 \leq \beta \\ 0 & \text{otherwise} \end{cases}$$

We design other oracle denoted by O'_f that is used to mark the retained elements of G :

$$|\alpha\rangle|\beta\rangle|i\rangle|j\rangle|\vec{f}_j\rangle|\vec{D}_i\rangle|0\rangle|(\vec{D}_i \bullet \vec{f}_j)^2\rangle \xrightarrow{O'_f} (-1)^{f'(i)} |\alpha\rangle|\beta\rangle|i\rangle|j\rangle|\vec{f}_j\rangle|\vec{D}_i\rangle|0\rangle|(\vec{D}_i \bullet \vec{f}_j)^2\rangle \quad (34)$$

Let $(B_{inner})^{-1}$ denote the inverse transform of B_{inner} .

Let $(U'_L)^{-1}$ denote inverse transform of U'_L .

Definition 15 By equations (32), (33) and (34), quantum 2-D DCT iteration G'_{DCT} is defined as

$$G'_{DCT} = (2|\xi'\rangle\langle\xi'| - I)(U'_L)^{-1}(B_{inner})^{-1}O'_f B_{inner}U'_L \quad (35)$$

, where $|\xi'\rangle = \frac{1}{N} \sum_{i=0}^{N-1} \sum_{j=0}^{N-1} \underbrace{|i\rangle|j\rangle}$.

B. Subroutine 2: Finding an Element $g_{i_0j_0} \in \{g_{ij} \mid \alpha \leq (g_{ij})^2 \leq \beta\}$

Subroutine 2 is similar to Subroutine 1.

Algorithm 16 Subroutine 2

Input parameters: α, β

Outputs: subscript (i_0, j_0) and corresponding coefficient $g_{i_0j_0}$; a global Boolean variable *IsSolution*.

Step1. Initialize $m = 1$ and $\lambda = \frac{6}{5}$; $IsSolution = FALSE$;

Step2. Choose j uniformly at random among the nonnegative integers not bigger than m .

Step3. Generate the initial state

$$|\Psi_0\rangle = \frac{1}{N} \sum_{i=0}^{N-1} \sum_{j=0}^{N-1} |\alpha\rangle|\beta\rangle \underbrace{|i\rangle|j\rangle}_{\text{registers}} |0\rangle|0\rangle|0\rangle|0\rangle$$

This can be achieved in $O(2 \log_2 N)$ steps using a $2 \lceil \log_2 N \rceil$ - bit Hadamard transformation.

Step4. Apply j iterations of G'_{DCT} starting from the state $|\Psi_0\rangle$. i.e.,

$$|\Psi_j\rangle = (G'_{DCT})^j |\Psi_0\rangle$$

Step5. Perform computation

$$|\Psi_{end}\rangle = B'_{inner} U'_L |\Psi_j\rangle$$

Step6. Observe the 3rd, 4th and 7th register: let (i_0, j_0) and coefficient $g_{i_0j_0}$ be the outcome respectively.

Step7. If $g_{i_0j_0} \in \{g_{ij} \mid \alpha \leq (g_{ij})^2 \leq \beta\}$, let $IsSolution = TRUE$, and *exit*; otherwise, go to step 8.

Step8. Set m to $\min\{\lambda m, N\}$ and go to step 2.

Similar to equation (28), Subroutine 2 has time complexity

$$Time(Subroutine2) = O\left(\frac{N}{\sqrt{t}}\right)t_M \quad (36)$$

where t is the number of elements in set $\{g_{ij} \mid \alpha \leq (g_{ij})^2 \leq \beta\}$.

C. Quantum 2-D DCT (QDCT2)

Algorithm 17 Quantum Algorithm to compute matrix G approximately

Input: The line vectors of matrix of D , that are stored in database with indices i (Figure 10);

The column vectors of matrix of F , that are stored in database with indices j (Figure 10);

Parameters: ΔE , α , β , threshold value $\varepsilon > 0$.

$nCount_i$ ($0 \leq i < N$): Counting the repeated times of coefficient c_i that is found when repeatedly applying subroutine 2.

$nMaxRepetition$: The maximum number of allowed repeated times of subroutine 2.

nS : The number of solutions that have been obtained.

Output: the big elements of G and corresponding indices $(i_0, j_0, g_{i_0 j_0})$, $(i_1, j_1, g_{i_1 j_1})$, \dots , $(i_R, j_R, g_{i_R j_R})$ such that $\frac{(g_{i_0 j_0})^2 + \dots + (g_{i_R j_R})^2}{\|F\|^2} \leq \varepsilon$. The other DCT coefficients are set to zero (Table 1).

Step0: $\Delta E = \|F\|^2 = \sum_{i=0}^{N-1} \sum_{k=0}^{N-1} (f_{ik})^2$; $\alpha = \frac{\Delta E}{N^2}$, $\beta = \Delta E$; $nS = 0$; $nCount_i = 0$, where $0 \leq i < N$.

By equation (1) and (2), $\|F\|^2 = \|\vec{f}_0\|^2 + \|\vec{f}_1\|^2 + \dots + \|\vec{f}_{N-1}\|^2$. That is, we can calculate $\|\vec{f}_0\|^2$, $\|\vec{f}_1\|^2$, ..., $\|\vec{f}_{N-1}\|^2$ one by one, then sum up these values. Thus,

$$Time(Step0) = Nt_I + (N-1)t_A + t_D \leq (5N+2)t_M + (N-1)t_A$$

while($\frac{\Delta E}{\|F\|^2} \geq \varepsilon$)

{

Step 1: Apply subroutine 2 to find a coefficient $(i_k, j_k, g_{i_k j_k})$;

Step 2: If $IsSolution = TRUE$ and $nCount_i = 0$,

then $\Delta E = \Delta E - (g_{i_k j_k})^2$, $nS = nS + 1$; $\alpha = \frac{\Delta E}{N^2 - nS}$, $\beta = \Delta E$; $nCount_{i_k} = nCount_{i_k} + 1$;

If $IsSolution = TRUE$, and $nCount_{i_k j_k} < nMaxRepetition$, continue;

If $IsSolution = TRUE$, and $nCount_{i_k j_k} \geq nMaxRepetition$, **exit** and apply classical algorithm to obtain DCT coefficients.;

If $IsSolution = FALSE$, **exit** and apply classical algorithm to obtain DCT coefficients.;

}

Algorithm 18 Quantum 2-D DCT (QDCT2) Applying the above algorithm, we will get the result of matrix G . Then compute 2-D DCT coefficients according to equation $C = GD$ (i.e., equation (30)) by using the same method. That is, applying the above method two times, we will obtain the 2-D DCT coefficients of image.

We can use classical method to compute the inverse DCT because many DCT coefficients is equal to zero so that many running times will be saved.

Similar to equation (29), Quantum 2-D DCT (QDCT2) has time complexity:

$$Time(QDCT2) = O(N)t_M \quad (37)$$

In contrast, the classical 2-D DCT has time complexity $O(N^2 \log_2 N)$ multiplications. Even the efficiency classical parallel 2-D DCT has time complexity $O(N \log_2 N) + Time(Communication)$, where $Time(Communication)$ denotes the communication time between processors [17]. Because many data will be shared by all processors, the communication time will drastically reduce the efficiency of parallel algorithm in fact [18]. By contrast, the there is no any communication time will be cost in Quantum 2-D DCT.

VI. THE COMPARISON BETWEEN THE QUANTUM DCT ITERATION AND THE GROVER ITERATION

The quantum DCT iteration $G_{DCT} = (2|\xi\rangle\langle\xi| - I)(U_L)^{-1}(O_{inner})^{-1}O_fO_{inner}U_L$ is derived from Grover iteration $G = (2|\Psi\rangle\langle\Psi| - I)O$. It includes two oracles; by contrast Grover's has only one oracle. In classical computer, complex computation must be decomposed into many simple function blocks (i.e., oracles) and then puts the function blocks back together to construct the complex computation. This is a necessary processing because complexity system is always constructed by many simple components. The law is also suitable to quantum computer maybe. Quantum DCT algorithm in this paper can do two things, which are simultaneously calculating DCT coefficients and simultaneously marking the wanted DCT coefficients. That is, complex computation has been decomposed into two oracles O_{inner} and O_f ; by contrast Grover's algorithm only can search a record with a given index. Equation (25) is the key of applying two or more oracles to perform complex computation. If there is no equation (25), applying two or more oracles is no significant (Fig13)

The method presented in this paper generalizes Grover's algorithm. The method is suitable to two or more arbitrary oracles. Clearly, if only if the iteration includes the unitary with the form $(\dots)^{-1}O_f(\dots)$ such that state is eigenstate with eigenvalue $(-1)^{f(i)}$, the method is valid.

The following table shows the difference between the quantum DCT iteration and the Grover iteration.

Insert Table 2 Here

VII. CONCLUSION

Discrete Cosine Transform (DCT) is very important in image compression. Almost all of digital films such as VCD and digital pictures such as JPEG files are compressed by utilizing DCT currently.

Real-time compressing and high compression ratio are the main research topics of image compression. The classical 1-D DCT has complexity $O(N \log_2 N)$ for N - dimensional vector. The time complexity of the classical 2-D DCT is $O(N^2 \log_2 N)$ for $N \times N$ image. In general, the more N is large, the more the compression ratio is high if the whole input data sequence is Markov chain and the order of chain is bigger than N . However, when N is large, classical DCT does not satisfy the requirement of real-time compressing. That is, finding a fast algorithm for large N is significant.

Quantum Fourier transform (QFT) and Klappenecker's Quantum DCT cannot be applied to image compression directly.

This paper presents the quantum DCT iteration G_{DCT} that is defined as $G_{DCT} = (2|\xi\rangle\langle\xi| - I)(U_L)^{-1}(O_{inner})^{-1}O_fO_{inner}U_L$. And constructs 1-D DCT based on the iteration with time complexity $O(\sqrt{N})$ for N - dimensional vector and quantum 2-D DCT with time complexity $O(N)$ for $N \times N$ image. Two properties of DCT is utilized to design the quantum DCT algorithm in this paper. One property is that DCT is energy conservation transform. The other property is that many of the DCT coefficients have values close to zero; these coefficients can be discarded without seriously affecting the quality of the reconstructed image.

In classical computer, complex computation must be decomposed into many simple function blocks (i.e., two or more oracles) and then puts the function blocks back together to construct the complex computation. The law is also suitable to quantum computer maybe. The quantum DCT iteration G_{DCT} includes two oracles so that it can perform more complex search; by contrast the Grover iteration $G = (2|\Psi\rangle\langle\Psi| - I)O$ has only one oracle so that it can only perform simple search. Most quantum algorithms have only one oracle currently, such as Shor's algorithm, Grover's algorithm, Simon algorithm, and Deutsch-Jozsa algorithm.

G_{DCT} is a rotation acting on subspace (Fig.14 and Fig15); by contrast, the Grover iteration acts on global space. Acting on subspace reduce search range drastically.

The method presented in this paper generalizes Grover's algorithm. Clearly, if only if the iteration includes the unitary with the form $(\dots)^{-1}O_f(\dots)$ such that state is eigenstate with eigenvalue $(-1)^{f(i)}$ (equation (25), Fig13), the method is valid. The method is universal and can be applied to discrete Fourier transform and other transforms for image compression.

Acknowledgement 19 *We thank Professor Z.-F. Han for his encouragement to us. We thank Yong-Jian Han, Pin-Xing Chen and Yun-Feng Huang especially for the significant discussing with them. We would also like to thank Yong-Shen Zhang, Ke-Hui Song, Guo-Ping Guo, Jian-Li, J.-M. Cai, M.-Y Ye, C. Han, Xiu -Ming Lin, Yu-liang Li, Huai Ye, and other colleagues for their help. We thank Prof. Jan-Zhang and Prof. Zhi-Lin Pu of Sichuan Normal Univ. for his help*

-
- [1] Rafael C. Gonzalez, Richard E. Woods, "Digital Image Processing," Publishing House of Electronics Industry ; Prentice Hall (Beijin, 2002)
 - [2] Wen Gao, 1994, "Technique of Multimedia Data Compression," Publishing House of Electronics Industry (Beijin: 1994)
 - [3] The help file of software MATLAB 7.0, May, 2004.
 - [4] Cheng Wang and Jia-Xin Song, "Computer Organization and Architecture," Tsinghua University publishers, China, 2004.
 - [5] Chao-Yang Pang, Zheng-Wei Zhou, Ping-Xing Chen, and Guang-Can Guo, "Design of Quantum VQ Iteration and Quantum VQ Encoding Algorithm Taking $O(\sqrt{N})$ Steps for Data Compression," Chinese Physics. (It will published on No. 15, Vol. 3, 2006 and will appear on March, 2006)
 - [6] M. A. Nielsen and I. L. Chuang, "Quantum Computation and Quantum Information," Cambridge University Press, Cambridge, 2000
 - [7] A. Galindo and M. A. Martín-Delgado, "Information and computation: Classical and quantum aspects," Reviews of Modern Physics, vol.74, April 2002
 - [8] A. Klappenecker and M. Rötteler, "Discrete Cosine Transforms on Quantum Computers," Proceedings of the 2nd International Symposium on Image and Signal Processing and Analysis, Pula, Croatia, June 19-21, 2001, S. Loncaric, H. Babic (eds.), pages 464-468, IEEE, 2001 (arXiv:quant-ph/0111038)
 - [9] Lov K. Grover, "A fast quantum mechanical algorithm for database search," Proceedings, 28th ACM symposium on Theory of Computing(STOC) , 1996, pp.212-218.

- [10] Eli Biham, et al., “Grover’s quantum search algorithm for an arbitrary initial amplitude distribution,” Phys. Rev. A 60, pp.2742-2745 , 1999
- [11] Eli Biham, et al., “Analysis of generalized Grover quantum search algorithms using recursion equations,” Phys. Rev. A 63, pp.012310:1-8 , 2000
- [12] Gui-Lu Long, ”Grover algorithm with zero theoretical failure rate,” PHYSICAL REVIEW A, VOLUME 64, 022307.
- [13] Gui-Lu Long, et.al., ”Phase Matching in Quantum Searching and the Improved Grover Algorithm,” Nuclear Physics Review, VoL.21, No.1, pp. 114-116, 2004
- [14] Michel Boyer, Gilles Brassard, Peter Høyer, Alain Tap, ”Tight bounds on quantum searching,” arXiv:quant-ph/9605034. (Journal-ref: Fortsch.Phys. 46 (1998) 493-506) , 1996
- [15] AI Kelley and Ira Pohl, ”Programming in C (Fourth Edition),” China Machine Press, China, 2004
- [16] Abraham Silberschatz, Peter Baer Galvin, ”Operating System Concepts (Fifth Edition),” John Wiley & Sons, Inc.,1997.
- [17] T. Bräunl, J.-S Li (translator), ”Parallel Image Processing,” Xian Jiaotong University Press, 2003.
- [18] Chao-Yang Pang, Ph.D thesis, ”Vector Quantization and Image Compression—The Analysis of Theory, The Design of Algorithm, Application and Implementation,” University of Electronic Science and Technology of China, Chengdu, China, 2002
- [19] Jose I. Latorre, ”Image compression and entanglement,” arXiv:quant-ph/0510031

VIII. LIST OF TABLES

Table 1: The 2-D DCT coefficients of left-top 8×8 blocks in image (a): Discards all but 10 of the 64 DCT coefficients in each block, and then reconstructs the image using the 2-D inverse DCT of each block. Although there is some loss of quality in the reconstructed image, it is clearly recognizable, even though almost 85% of the DCT coefficients were discarded. This property is utilized to design quantum algorithm in this paper

4.9211	-0.00773	0.002581	0.001847	...	0
0.014981	-0.00281	0.002071	0	...	0
0.008015	0.002014	0	0	...	0
-0.0196	0	0	0	...	0
⋮	⋮	⋮	⋮	⋮	⋮
0	0	0	0	0	0

Table 2: The Comparison between quantum DCT iteration and the Grover iteration



FIG. 1: The image with size 128×128 is represented by the right 128×128 matrix . Each element of this matrix is called *pixel*. The pixel value f_{ij} is a gray-level value. The value f_{ij}^2 is proportional to brightness or energy. The more f_{ij} is large, the more corresponding point in image is bright.



FIG. 2: 256×256 image.

$G_{DCT} = (2 \xi\rangle\langle\xi - I)(O_{inner}U_L)^{-1}O_f(O_{inner}U_L);$ $G = (2 \Psi\rangle\langle\Psi - I)O$
$(U_L)^{-1}(O_{inner})^{-1}O_fO_{inner}U_L \alpha\rangle \beta\rangle i\rangle \vec{f}\rangle 0\rangle 0\rangle 0\rangle$ $= (-1)^{f(i)} \alpha\rangle \beta\rangle i\rangle \vec{f}\rangle 0\rangle 0\rangle 0\rangle;$ $O i\rangle = (-1)^{f(i)} i\rangle$
G_{DCT} has two oracles O_{inner} and O_f ; G has only one oracle
G_{DCT} is a rotation on subspace; G is a rotation on global space.
G_{DCT} can perform more complex search; G only can perform simple search
The method presented in this paper generalizes the Grover iteration.

IX. LIST OF FIGURES



FIG. 3: reconstructed image

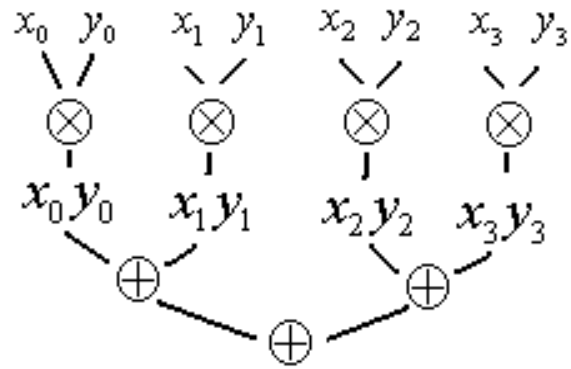


FIG. 4: The Parallel Circuit for Computing Inner Product: when $N \leq 2^{4 \times 25}$, $t_I \leq 5t_M$

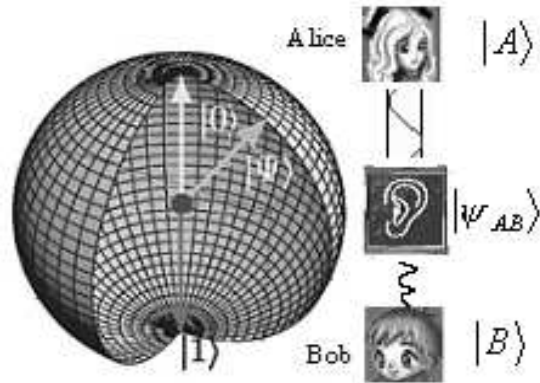


FIG. 5: The schematic diagram of the analogies between quantum superpositions and sonic wave.

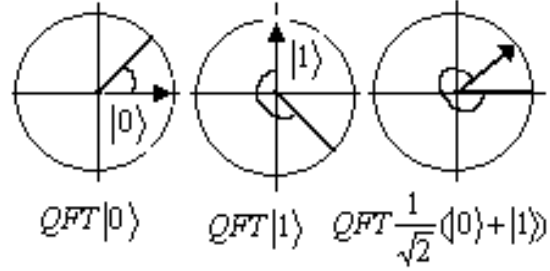


FIG. 6: QFT only acts on basis states $|0\rangle$ and $|1\rangle$: $QFT\frac{1}{\sqrt{2}}(|0\rangle+|1\rangle) = \frac{1}{\sqrt{2}}(QFT|0\rangle+QFT|1\rangle)$

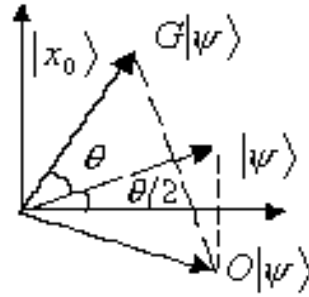


FIG. 7: The schematic diagram of rotating the state $|\Psi\rangle$ by θ radians per application of G

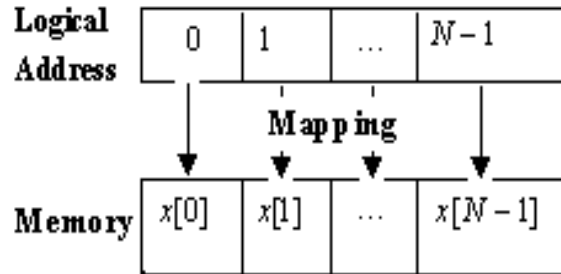


FIG. 8: The Conception of the Logical Mapping. The mapping associates data with the corresponding logical address

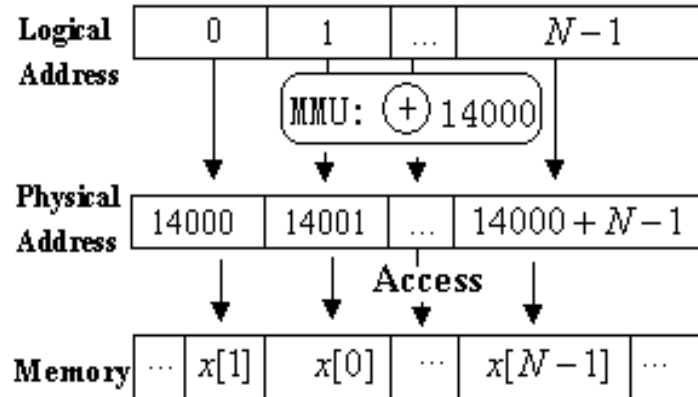


FIG. 9: The Illustration of the Physical Realization of the Logical Mapping [16]. Accessing data is very very fast operation so that the time of access can be ignored when designing algorithm.

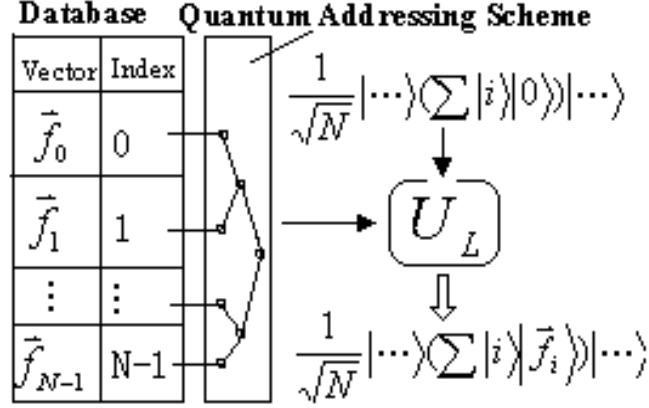


FIG. 10: The Representation of Image by Using Quantum States: LOAD operation $U_L : |i\rangle|0\rangle \xrightarrow{U_L} |i\rangle|0 \oplus \vec{f}_i\rangle$ is a CNOT operation and is a very very fast operation so that the time of addressing can be ignored when designing quantum algorithm such as Grover's algorithm. It is clear that the most efficient possible algorithm is in this model of computation

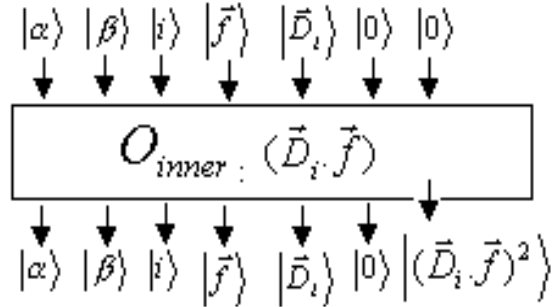


FIG. 11: The Conception of Oracle O_{inner}

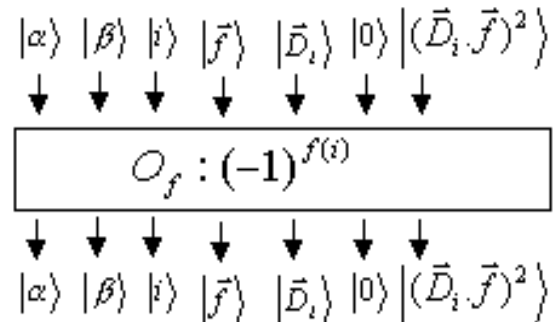


FIG. 12: The Conception of Oracle O_f

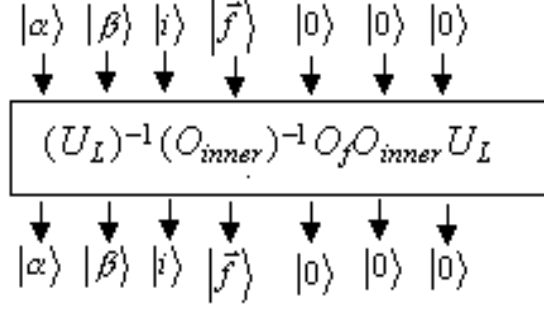


FIG. 13: $(U_L)^{-1}(O_{inner})^{-1}O_fO_{inner}U_L$ only changes the phase of the state as $(-1)^{f(i)}$. This is a key of applying two or more oracles to perform complex search.

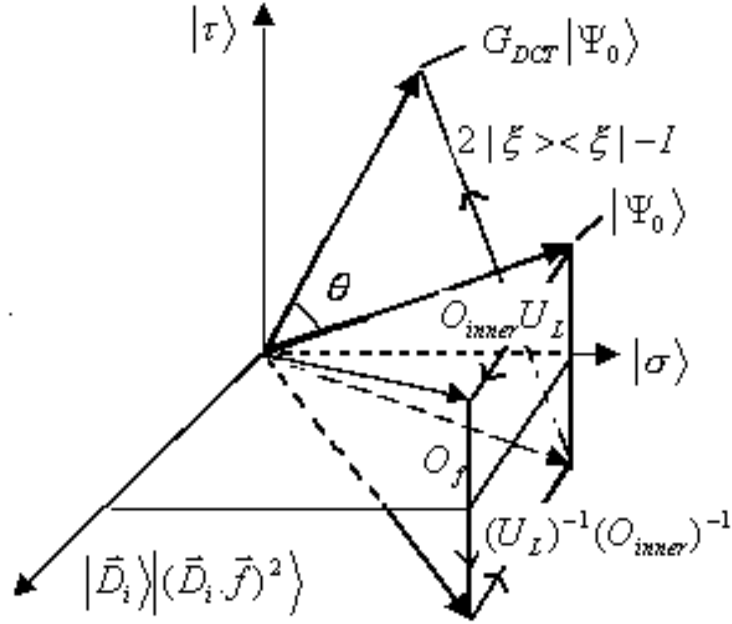


FIG. 14: The Action of A Single Quantum 1-D DCT Iteration G_{DCT} : The initial state $|\Psi_0\rangle$ is rotated in the subspace $span\{|i\rangle\}$ by θ towards the superposition $|\tau\rangle$ of all solutions to the search. Initially, it is inclined at angle $\frac{\theta}{2}$ from $|\sigma\rangle$, a state orthogonal to $|\tau\rangle$. The product operation $(U_L)^{-1}(O_{inner})^{-1}O_fO_{inner}U_L$ reflects the state about the state $|\sigma\rangle$, then the operation $2|\xi\rangle\langle\xi| - I$ reflect it about $|\xi\rangle$ in the subspace $span\{|i\rangle\}$.

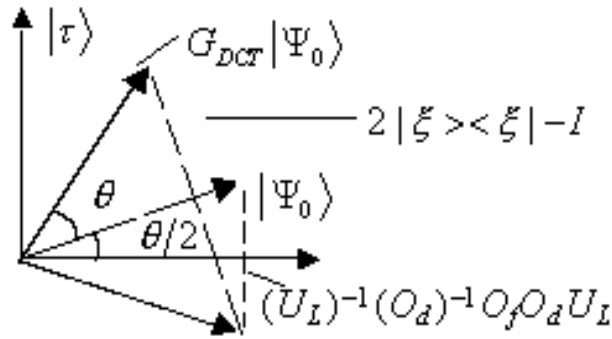


FIG. 15: G_{DCT} is equivalent to a rotation on subspace $span\{|i\rangle\}$

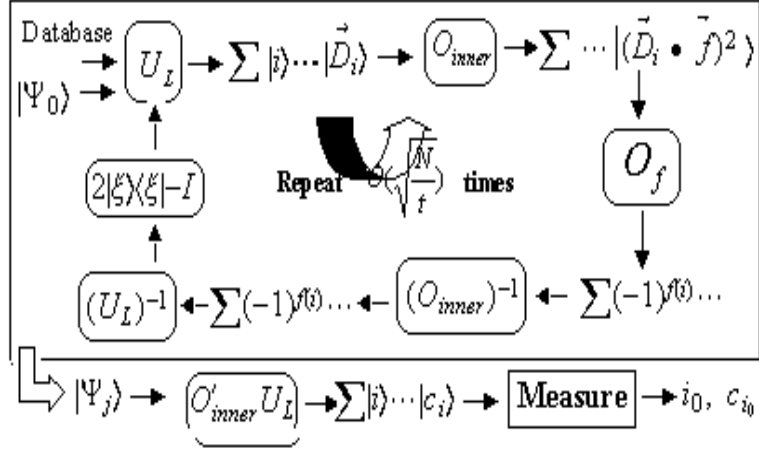


FIG. 16: Schematic processing of subroutine 1

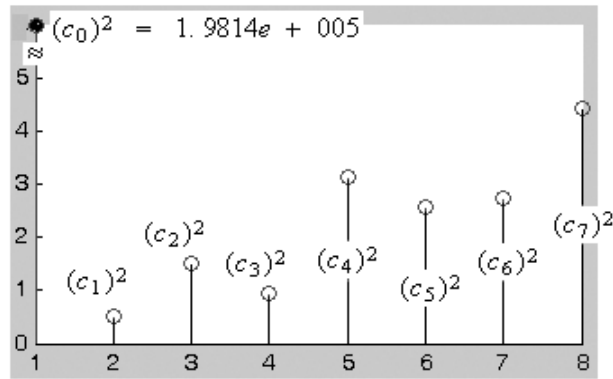


FIG. 17: Solution Set: $S = \{c_0\}$. The output is $(0, c_0)$.

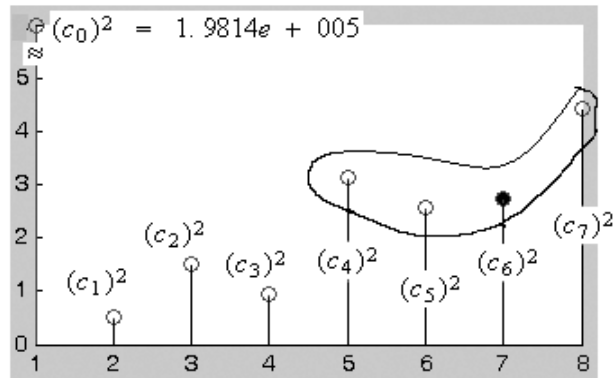


FIG. 18: Solution Set $S = \{(4, c_4), (5, c_5), (6, c_6), (7, c_7)\}$. We will obtain one of solution with equal probability. The output is $(6, c_6)$